Asian Journal of Chemistry; Vol. 37, No. 3 (2025), 617-623

ASIAN JOURNAL OF CHEMISTRY

https://doi.org/10.14233/ajchem.2025.33250

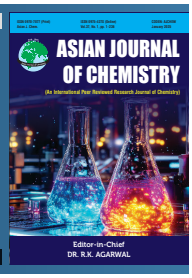

Synthesis and Characterization of Cobalt(II) Complex of Polyamido-Amine (PAMAM) Decorated Azomethine Ligand: *In Vitro* Biological Evaluation

R.Y. PATLE[1,2,*], Y.N. SELOKAR[3], K.K. MESHRAM[1] and R.S. DONGRE[1]

[1]PGTD Chemistry, Rashtrasant Tukadoji Maharaj Nagpur University, Nagpur-440033, India
[2]Department of Chemistry, Mahatma Gandhi College of Science, Gadchandur, Chandrapur-442908, India
[3]Department of Molecular Biology and Genetic Engineering, Rashtrasant Tukadoji Maharaj Nagpur University, Nagpur-440033, India

*Corresponding author: E-mail: ramkrishnapatle1986@gmail.com

Received: 23 December 2024; *Accepted*: 4 February 2025; *Published online*: 28 February 2025; AJC-21918

A new cobalt(II) complex based on polyamido-amine (PAMAM) dendrimer was modified with 2-hydroxy-3-methoxybenzaldehyde. The structural elucidation of synthesized ligand and its complex were performed by the FTIR, NMR, Mass, EDX, TGA/DTA and UV-Vis analyses. The *in vitro* antimicrobial investigation of the synthesized complex was performed against Gram-positive *Staphylococcus aureus*, Gram-negative *Escherichia coli* bacterial strains and fungal strain *Candida albicans* by well-diffusion method. The antibiotic tetracycline (10 mg/mL) for antibacterial and fluconazole antibiotic for antifungal potency were used as reference standard. The results have revealed that the PAMAMM-G0-OV-Co(II) complex has shown excellent inhibitory antibacterial action against *S. aureus* with highest zone of inhibition of 16 mm and *E. coli* with highest zone of inhibition of 21 mm at 10 mg/mL of concentration. Similarly, the complex has shown exceptional antifungal activity with average zone of inhibition of 15 mm against *Candida albicans* fungal strain. Thus, the dendritic cobalt complex has shown antibacterial and antifungal activity at a considerable level at 10 mg/mL concentration.

Keywords: Cobalt(II) complex, PAMAM dendrimer, Antimicrobial activity, Schiff bases.

INTRODUCTION

Dendrimers are multi-faceted nano-architectures known for their vast applications in all dimensions such as biomedical, environmental remediation, catalysis and molecular probes [1]. The significant role of dendrimers in the biomedical domain cannot be ignored as it has demonstrated their applicability due to their unique properties. The dendrimers are characterized by their nano-size, three-dimensional globular shape with tree-like branching own inner voids and modifiable surface active functionalities [2]. Amid the dendrimer family, poly(amido-amine) dendrimer is the innovative discovery of Tomalia *et al.* [3] who first introduced it as starburst dendritic polymer. PAMAM dendritic architecture is featured by internal amide (-CONH-) and peripheral amine ($-NH_2$) groups. The topology of PAMAM dendrimer becomes more complex as it grows from lower generation (G0) to higher generation (G10) meanwhile it confers several internal voids in the structure [4]. PAMAM dendrimer offers surface modification *via* conjugation of the suitable moiety to formulate the novel hybrid as per the applicability in the biomedical fields. The recent literature has revealed that PAMAM dendrimers are modified with the PEG, acetyl moiety, biotin, *etc.* to enhance the drug delivery capability in cancer treatment by reducing its cytotoxicity for normal human cells [5-9]. Furthermore, the peripheral amine groups of PAMAM are more susceptible to yield the Schiff bases with aldehydes and ketones [10,11]. PAMAM dendrimer having surface amine functionalities is prepared with salicylaldehyde to yield the Schiff base and employed for environmental remediation [12,13].

Thus, the azomethine functionality of Schiff base is well recognized for coordinating the transition metals to yield stable complexes. The Schiff bases and their coordinated metal complexes are widely employed as antioxidant, antiviral, anticancer, antimicrobial, antiproliferative and anti-inflammatory agents [14-20]. Similarly, Schiff bases are the prominent bioactive molecules that yielded stable metal complexes with metals such as UO_2^{2+}, Zn^{2+}, Fe^{3+} and Cu^{2+}, which displayed excellent inhibitory properties on bacterial strains [21]. The Schiff base ligand

1,8-naphthalimide anchored with *o*-vanillin coordinated with Co^{2+} yielded naphthalimide cored metal complex was evaluated against bacterial strains and found to be effective antibacterial agents against Gram-positive and Gram-negative strains [22]. Schiff base derived from 3-amino-4-hydroxybenzenesulfonic acid and vanillin forming a metal complex with Co^{2+}, Cu^{2+}, Ni^{2+} and Zn^{2+} were investigated for antimicrobial activity have shown the significant minimum inhibitory concentration which exhibited the higher antimicrobial appraisal [23]. The Cu(II) metallo-dendrimer Schiff base complex of PAMAM modified with 1,8-naphthalimide unit also exhibited considerable antibacterial activity against the bacterial strains [24].

The current research work is focused on the synthesis of the cobalt(II) complex of PAMAM decorated with 2-hydroxy-3-methoxybenzaldehyde Schiff base ligand and characterized by spectroscopic and analytical techniques. The synthesized complex was also evaluated for the antimicrobial assessment against Gram-positive and Gram-negative bacterial and also fungal strains to reveal the biological potency of the synthesized complex.

EXPERIMENTAL

Analytical grade chemicals such as $CoCl_2 \cdot 6H_2O$, ethanol, methanol, diethyl ether, 2-hydroxy-3-methoxybenzaldehyde (OV) and distilled water were purchased from Sigma-Aldrich and Merck, India. PAMAM-G0 dendrimer synthesized in laboratory as described elsewhere [25].

Characterization: The ^1H and ^{13}C NMR were analyzed using Bruker AVANCE NEO 500 MHz FT-NMR spectrometer, Mass was recorded using MALDI-TOF Synapt XS HD mass spectrometer. The FTIR was recorded using a spectrometer (Shimadzu, Japan) and XRD was performed on a Rigaku (Miniflex 600) X-ray diffractometer. Thermal analysis was performed using a DTG-60 simultaneous DTA/TG instrument (Shimadzu, Japan) at a scan rate of 20 ºC/min and a nitrogen flow rate of 100 mL/min. SEM-EDX analysis was performed on the Jeol 6390LA/OXFORD XMX N instrument at an accelerating voltage of 0.5 kV to 30 kV and the element composition was analyzed using the CHNS Analyser (model: ELEMENTAR Vario EL III). The electronic spectrum was determined using a Shimadzu UV-VIS spectrophotometer.

Synthesis of PAMAM-G0-OV ligand (L): In two-necked round bottom flask, 2-hydroxy-3-methoxybenzaldehyde (OV, 4 mmol) and PAMAM G0 dendrimer (1 mmol) were reacted in 50 mL of ethanol and a catalytic amount of glacial acetic acid was added to the reaction mixture. The mixture was sonicated for 1 h and then stirred at room temperature for 12 h. The completion of the reaction was monitored by TLC chromatography. After completion of the reaction, a viscous compound was obtained by solvent evaporation followed by washing with diethyl ether (**Scheme-I**). The product was kept 24 h for under a vacuum to remove the extra solvent. FTIR (KBr, cm^{-1}): 3360 ν(OH), 3291 ν(N–H), 2930, 2838 ν(aliphatic C–H), 1631 ν(C=N), 1539 ν(ArC=C), 1455 ν(ArC–C), 1240 ν(ArC–O). ^1H NMR (500 MHz, $CDCl_3$, TMS, δ ppm): 2.23-3.71 (m, 20H, CH_2), 3.91 (s, 12H, CH_3O), 6.72-7.30 (m, 16H, Ar–H), 8.14 (s, 4H, CH=N); 8.51 (s, 4H, NH); 5.41 (s, 4H, –OH). ^{13}C NMR (125 MHz, $CDCl_3$, δ ppm): 31.42, 33.64, 36.48, 40.09, 55.95, 57.49, 114.15, 118.44, 123.26, 148.56, 152.91, 162.59, 166.40, 172.96. LC-MS (TOF MS ESI) for $C_{54}H_{72}N_{10}O_{12}$ (*m/z*): 1053 $[M+1]^+$.

Synthesis of PAMAMG0-OV-Co(II) complex (ML): Cobalt(II) chloride was dissolved in 20 mL of methanol and slowly added to the Schiff base dissolved in 30 mL of methanol (M:L = 2:1 ratio). The reaction mixture was refluxed for 12 h with stirring. The reaction mixture was cooled at 0 ºC for 24 h. The dark green precipitate obtained was washed with diethyl ether and dried the product (**Scheme-II**).

Antimicrobial study: Cobalt(II) complex was assayed against Gram-positive bacteria *Staphylococcus aureus,* Gram-

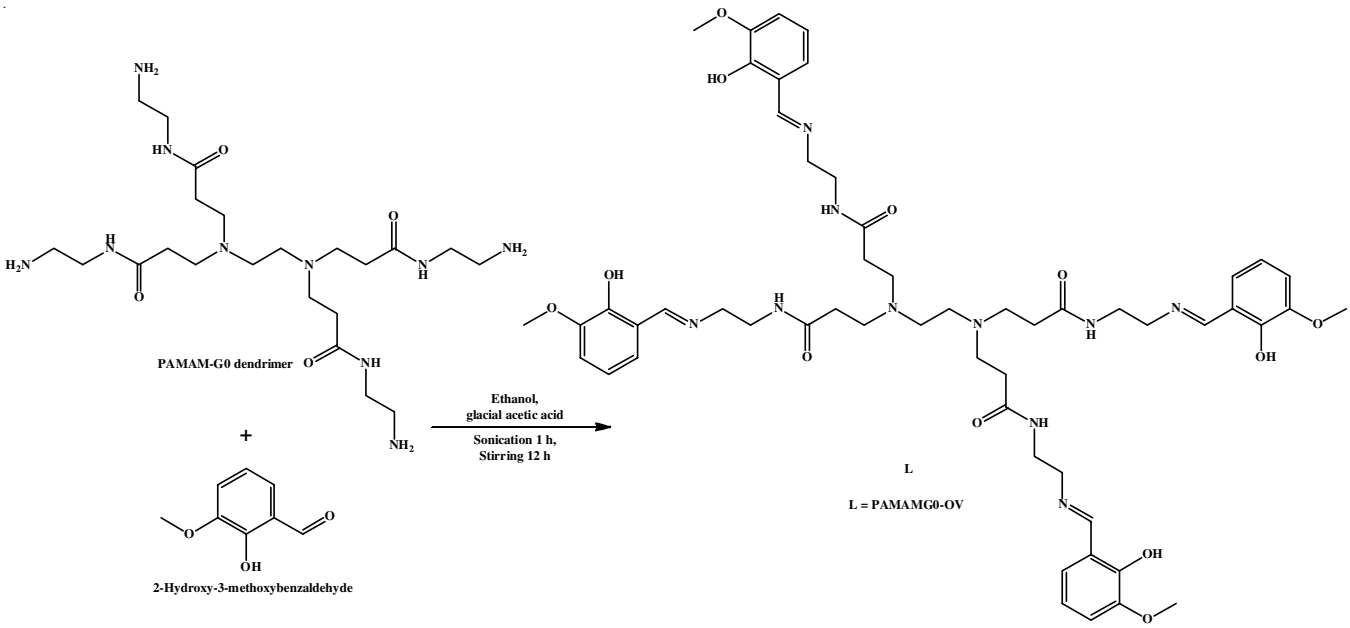

Scheme-I: Synthesis of the Schiff base ligand (L)

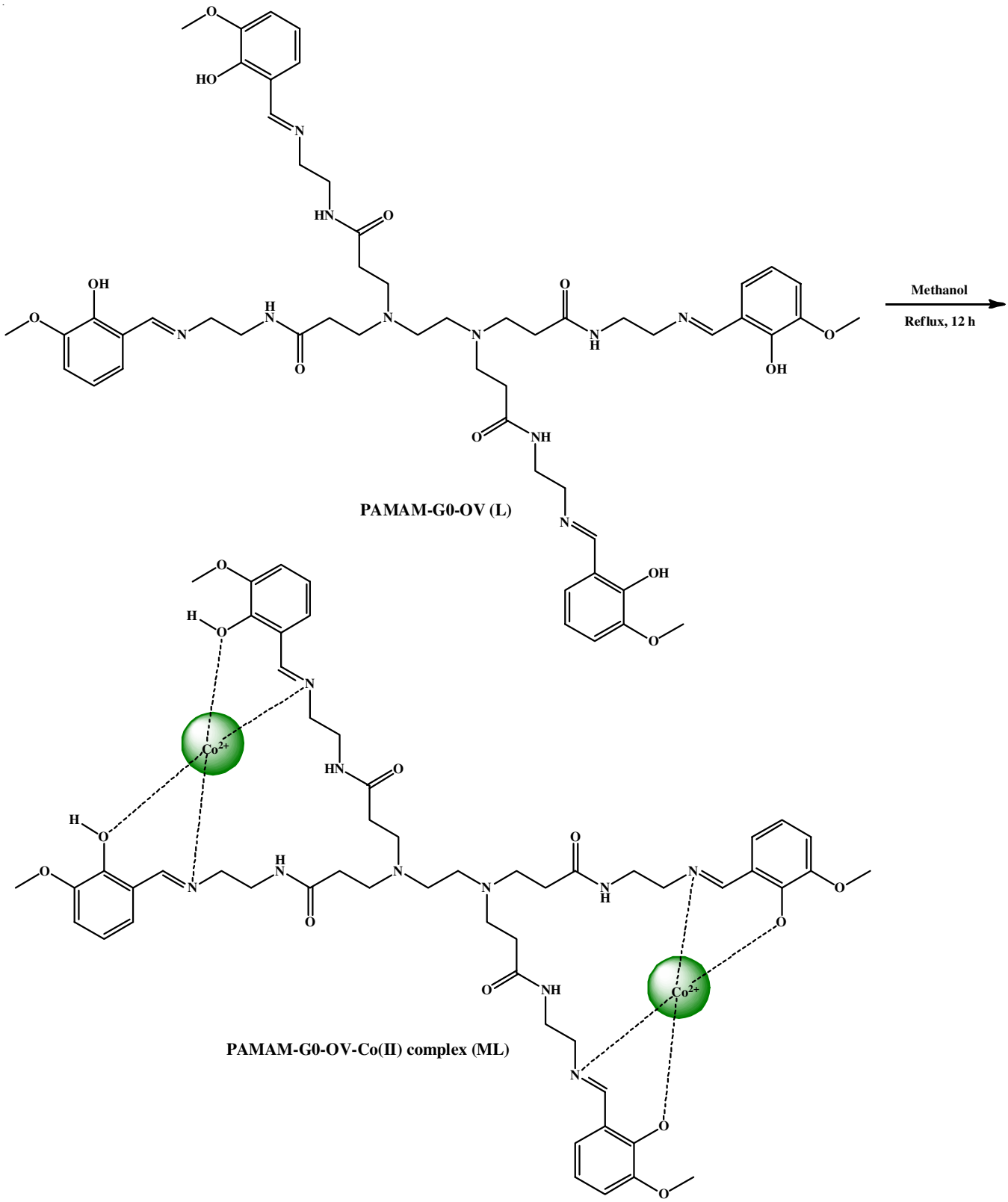

Scheme-II: Synthesis of PAMAMG0-OV-Co(II) complex (ML)

negative *Escherichia coli* and fungal strain *Candida albicans* by well diffusion method. The Mueller-Hinton agar (MHA) plates were prepared and culture was grown on the tryptic soy broth (TSB) nutrient broth. The MHA agar plate was inoculated with the bacterial strain and the sample was prepared at a concentration of 1 mg/mL, 5 mg/mL and 10 mg/mL in DMSO solvent. Similarly, the antifungal activity was performed on the potato dextrose agar (PDA) plate against fungal strain. Then sample, antibiotic as the reference standard and DMSO as blank were placed in the well for the diffusion. The plates were then

incubated at 37 ºC for 24 h for antibacterial and 72 h for antifungal activity. After the completion of incubation period and then the zone of inhibition (ZOI) was measured.

RESULTS AND DISCUSSION

FTIR spectral studies: FT-IR spectra of PAMAM G0-OV ligand (L) and its Co(II) complex are represented in Fig. 1. In the spectra, the absorption peak at 3291 cm^{-1} is attributed to the overlap frequency of the phenolic –OH and dendritic –NH- groups. Additionally, the peak at 3071 cm^{-1} was attributed to –CH- stretching of the aromatic ring of *o*-vanillin. The $–CH_2$- stretching vibration at 2930 cm^{-1} is obtained. Azomethine (-CH=N-) strongly absorbs at 1631 cm^{-1} while the peaks at 1455 cm^{-1} and 1539 cm^{-1} are associated with ring vibration. The spectra represent sharp bands with higher intensity peaks of functional groups of Schiff base ligand, meanwhile ML complex represents the broad peaks with lower intensities of –OH and -CH=N- groups due to the coordination of Co^{2+} ions with the donor O and N atoms of the functional groups of the Schiff base ligand moiety. Thus, the complexation of ligand with Co(II) ion involves mainly coordination of -CH=N- and –OH functionalities with the metal ion.

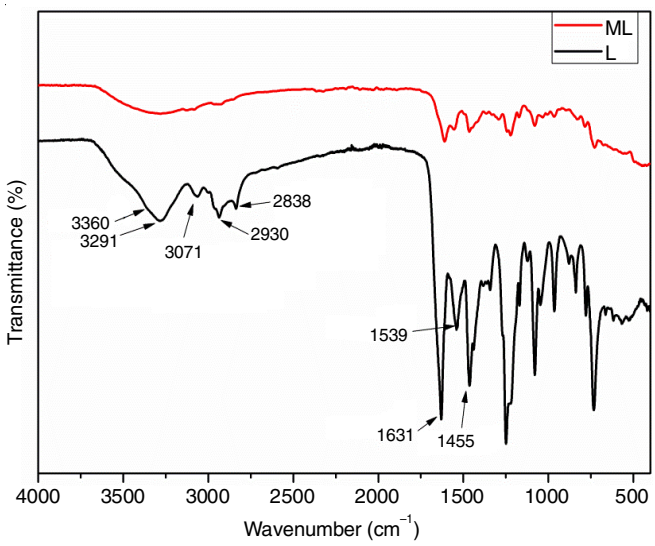

Fig. 1. FTIR spectra of PAMAMG0-OV ligand (L) and its Co(II) complex (ML)

NMR spectral studies: The ^1H and ^{13}C NMR spectra of ligand (L) are represented in Fig. 2. The characteristic signals of aliphatic CH_2 protons appeared around the ligand observed at δ 2.23-3.71 ppm. The signal at δ 3.91 ppm belongs to $–OCH_3$ protons. The benzene ring attached C-**H** protons signals are observed at around δ 6.72-7.30 ppm. The characteristics signal at δ 8.14 ppm corresponds to the azomethine (C**H**=N) proton while the signal at δ 8.51 ppm is attributed to the N**H** proton of the amide functional group. The phenolic OH proton signal is observed at δ 13.7 ppm [26]. Similarly, ^{13}C NMR spectrum of ligand display the highest signal at 172.96 which is attributed to carbon attached to oxygen atoms in the carbonyl (C=O) functional group. The carbon of the azomethine (HC=N) group appeared at δ 166.40 ppm while the signal at δ 162.59 ppm represents the ring carbon directly attached to the phenolic hydroxyl (Ar-OH) group. The other signals at δ 152.91 and δ 148.56 ppm correspond to ring carbon directly attached to the methoxy ($-OCH_3$) and azomethine groups respectively. Moreover, the signal corresponding to methoxy carbon is obtained at δ 57.49 ppm and methylene carbons appeared at around δ 31.42-55.95 shift. The ^1H and ^{13}C NMR spectra displayed the characteristics signals which support the successful synthesis of ligand.

MS spectral studies: The MS spectra of the PAMAM-G0-OV ligand and its cobalt(II) complex are represented in Fig. 3. The molecular ion peaks of ligand are obtained at *m/z* 1053 which is attributed to $(M+1)^+$ and the molecular complex ion $[M+Co_2]^+$ peak with maximum abundance is observed at around *m/z* 1167.4, 1168.4 and 1169.4, which are closed to the calculated mass of *m/z* 1170. The other characteristic fragmentations are obtained at *m/z* 1223.4, 1224.4 and 1225.4 which are assigned to the $[M+Co_2+Cl+H_2O]^+$. There are diversified fragmentations observed in the spectra supporting the successful synthesis of ligand and complex.

UV-vis spectral studies: The UV-vis spectra of PAMAM Schiff base ligand and its cobalt(II) complex are presented in Fig. 4. The electronic spectra of the ligand and its complex were analyzed using DMSO solvent. The higher polarity DMSO

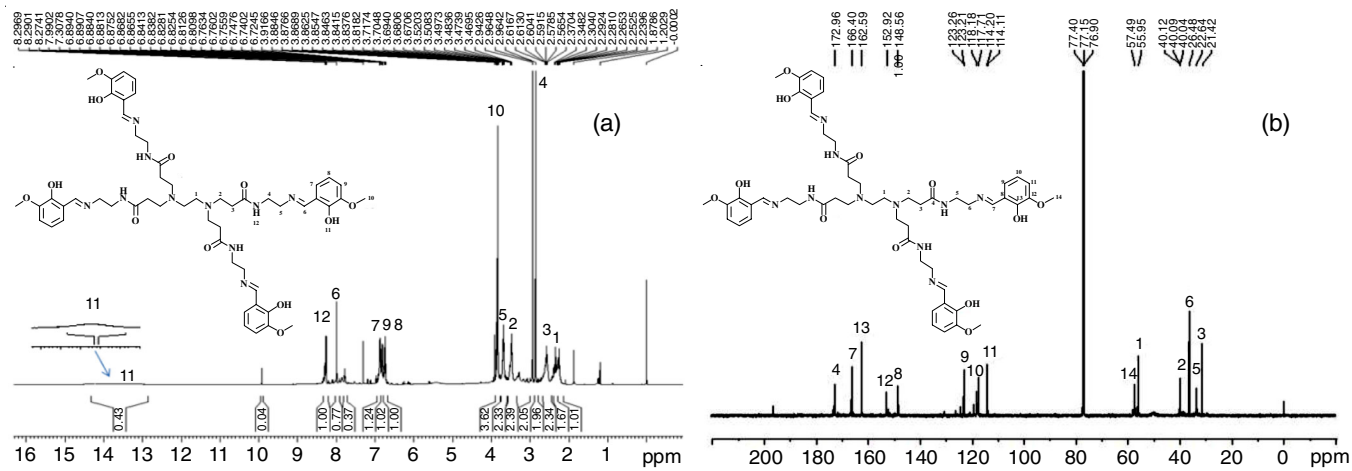

Fig. 2. (a) ^1H NMR and (b) ^{13}C NMR spectra of PAMAMG0-OV ligand (L)

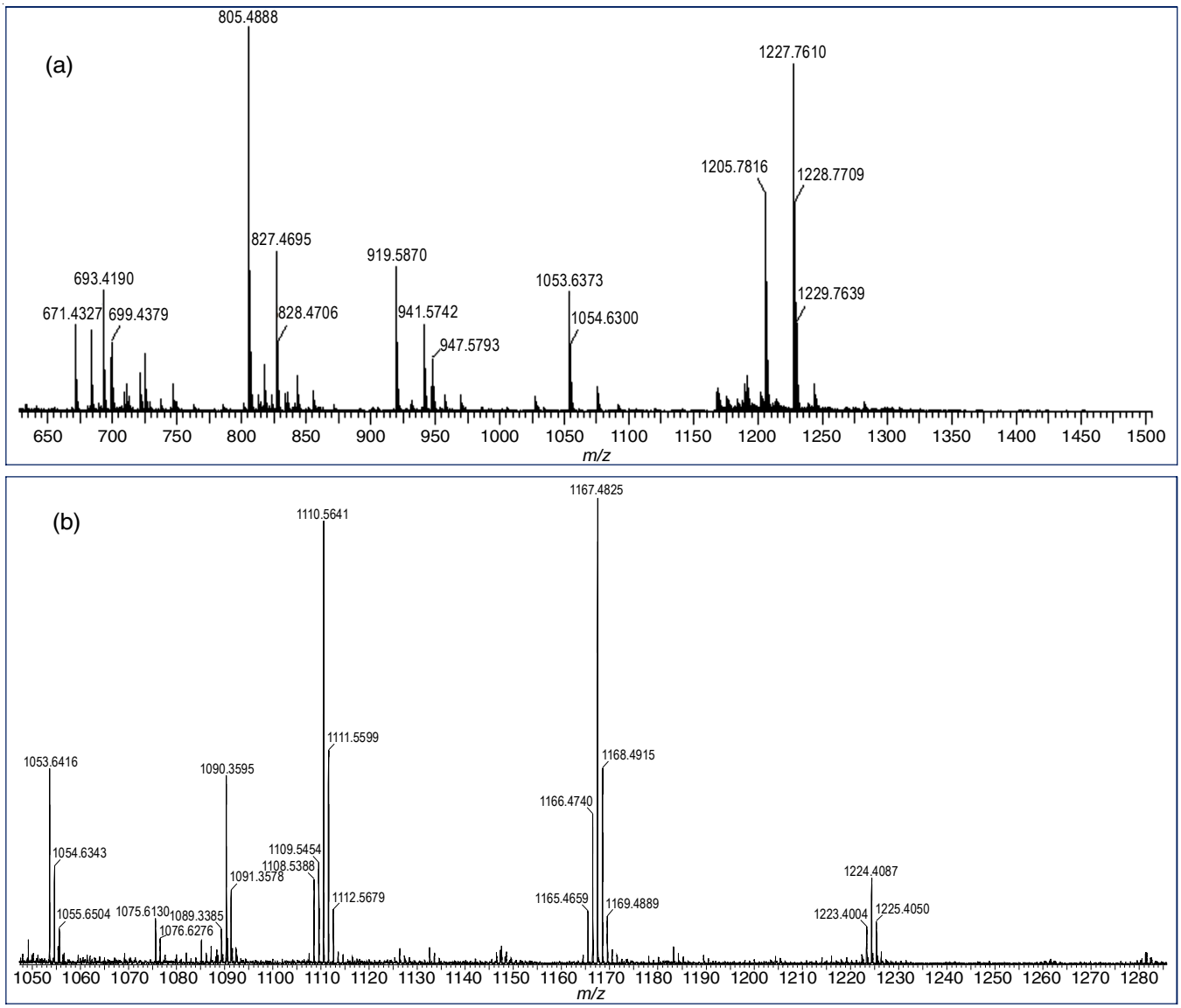

Fig. 3. (a) MS spectrum of PAMAMG0-OV ligand (L) and (b) MS spectrum of PAMAMG0-OV-Co(II) complex

conferred a strong interaction with solute and the absorption bands appeared at longer wavelengths. In the dendritic Schiff base ligand, five absorption bands were observed. For the carbonyl group of ligand, the absorption bands at 224 nm and 355 nm correspond to $\pi \rightarrow \pi^*$ and $n \rightarrow \pi^*$ transition, respectively. Similarly, for the azomethine (-CH=N-) group of ligand, the absorption bands at 329 nm and 405 nm correspond to the $\pi \rightarrow \pi^*$ and $n \rightarrow \pi^*$ transitions, respectively. The characteristics B-band of the benzene ring were observed at 260 nm in the spectra. After the formation of Co(II) metal complex, the coordinate-covalent bonding between the ligand and metal ion resulted in the blue shift of absorption bands, which is attributed to $n \rightarrow \pi^*$ transition of both carbonyl and azomethine from 355 nm to 274 nm and 405 nm to 380 nm, respectively while B-band of the benzene ring occurred slightly blue shift from 260 nm to 230 nm. The UV-Vis spectra demonstrated the successful synthesis of metal-ligand (ML) complex [27].

EDX analyses of complex: The EDX spectra of the complex are displayed in Fig. 5. The EDX spectra of the ML

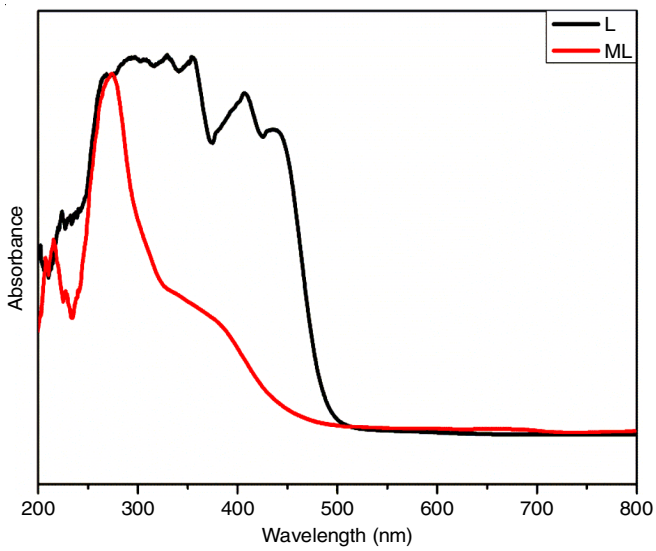

Fig. 4. UV-Vis spectra of PAMAMG0-OV ligand (L) and PAMAMG0-OV-Co(II) complex (ML)

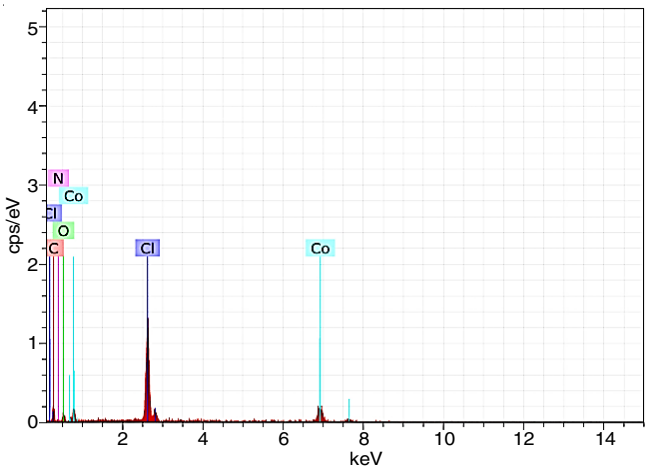

Fig. 5. EDX spectrum of PAMAMG0-OV-Co(II) complex (ML)

complex exhibited prominent peaks of elements present in the complex. The Kα X-ray emission from the Co, Cl, N, C and O appeared at high-intensity peaks with different energy (keV). The spectrum exhibited two peaks at higher and lower energy (keV) for Co and Cl atoms. The appearance of characteristic peaks in the spectrum indicates the formation of the Co(II) metal complex with the PAMAM-G0-OV ligand.

TGA/DTA studies: Thermal gravimetric analysis (TGA) of the synthesized compound is represented in Fig. 6. TGA/DTA curves are discussed in three stages A, B and C namely drying, pyrolysis and carbonization stage, respectively. Stage A characterized by the drying stage accompanied by loss of moisture at 100 ºC with 10% loss of weight. The second stage B is characterized by pyrolysis which starts at 101 ºC and completed at 650 ºC. It is accompanied by the 46% weight loss associated with the decomposition of organic moiety such as Schiff base ligand and the release of gases such as ammonia, chlorine, carbon dioxide, *etc*. The third stage C is called the carbonization stage which is characterized by 60% weight loss of up to 900 ºC. The actual disintegration of the complex started at 250 °C to 650 °C which involved maximum weight loss. Thus, TGA/DTA results demonstrated the considerable stability of the PAMAMG0-OV-Co^{2+} complex (ML).

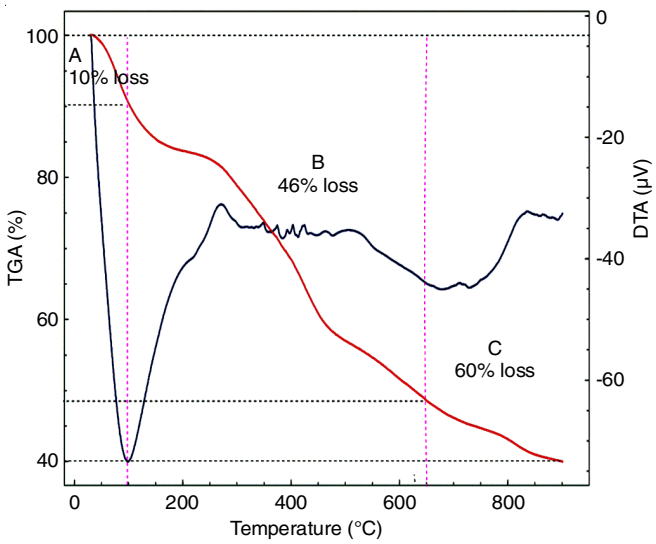

Fig. 6. Thermograms of PAMAMG0-OV-Co(II) complex (ML)

Antimicrobial activities: The synthesized Co(II) dendimer complex against Gram-positive (*S. aureus*), Gram-negative (*E. coli*) bacterial strains and fungi strains (*C. albicans*) exhibited significant activity. The PAMAM-G0-OV-Co(II) complex exhibited significant antifungal activity against *C. albicans* and moderate against bacterial strains (Table-1). The antibiotic tetracycline used as a reference has shown the highest anti-bacterial and antifungal performance than the complex. The highest inhibitory action of the complex is observed at a 10 mg/mL against *S. aureus* while at all concentrations in *E. coli*. The fungal strain *C. albicans* was inhibited at 5 mg/mL and 10 mg/mL concentration (Fig. 7a). The tetracycline used as a reference has shown highest inhibitory action than the complex against bacterial and fluconazole against fungal pathogens (Fig. 7b).

Conclusion

The newly synthesized PAMAM-G0-OV Schiff base ligand cobalt(II) metal complex was characterized by various spectro-analytical techniques to elucidate the structure of the Co(II) complex. The synthesis of the PAMAMG-OV ligand

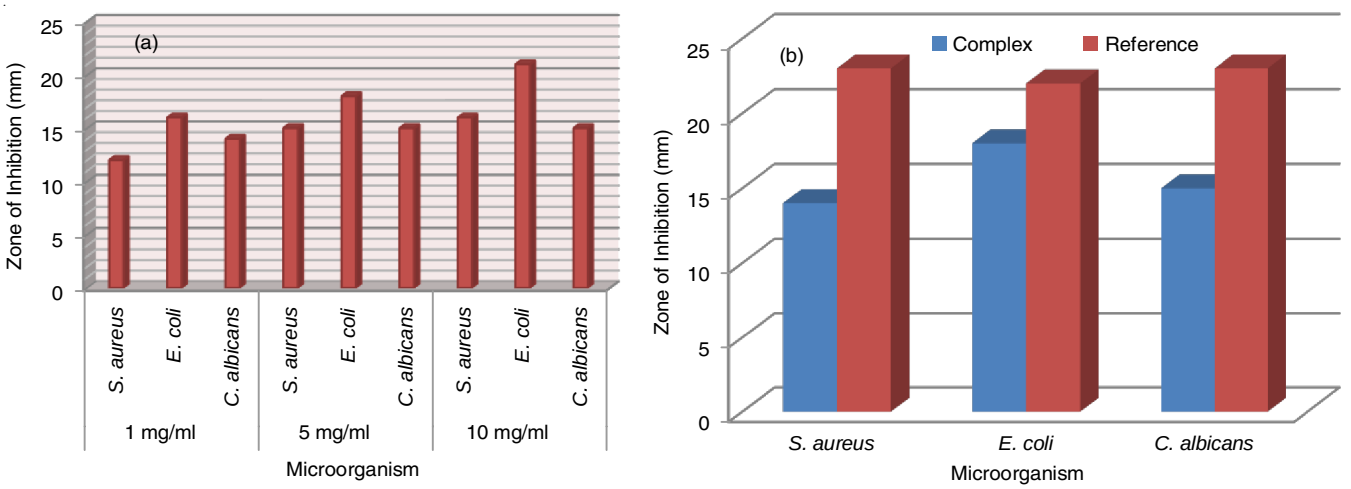

Fig. 7. Antimicrobial activity of (a) PAMAM-G0-OV-Co(II) complex (ML) at different concentrations and (b) PAMAMG0-OV-Co(II) complex (ML) and reference antibiotic against pathogens

TABLE-1
ZONE OF INHIBITIONS OBTAINED AGAINST BACTERIAL AND FUNGAL PATHOGENS

Microorganism	Zone of inhibition (mm)				
	Control (DMSO)	Reference standard (tetracycline/fluconazole)	ML complex		
			1 mg/mL	5 mg/mL	10 mg/mL
S. aureus	0	25	12	15	16
E. coli	0	22	16	18	21
C. albicans	0	24	14	15	15

and its Co(II) complex was confirmed by ^{1}H and ^{13}C NMR, FTIR, UV-Vis, Mass, EDX and TG analysis. Two Co(II) ions are coordinated to the ligand molecule by phenolic hydroxyl (-OH) and azomethine (HC=N-) of the ligand with donor atoms O and N. The complex was examined for the antibacterial and antifungal appraisal at concentrations of 1 mg/mL, 5 mg/mL and 10 mg/mL of sample in DMSO. The compound at 10 mg/mL concentration has shown highest antimicrobial effects. The Co(II) complex was severely active against *S. aureus* and *E. coli* with the highest zone of inhibition of 16 mm and 21 mm respectively. However, it was strongly active against *Candida albicans* fungal strain having average zone of inhibition of 15 mm.

ACKNOWLEDGEMENTS

The authors are grateful to The Head of the Department, R.T.M. Nagpur University, Nagpur, India for providing the research facilities. The authors also acknowledge the SAIF Chandigarh and SAIF-RTM Nagpur University, Nagpur for providing characterization facilities.

CONFLICT OF INTEREST

The authors declare that there is no conflict of interests regarding the publication of this article.

REFERENCES

1. F. Najafi, M. Salami-Kalajahi and H. Roghani-Mamaqani, *J. Iran. Chem. Soc.*, **18**, 503 (2021); https://doi.org/10.1007/s13738-020-02053-3
2. R.J. Smith, C. Gorman and S. Menegatti, *J. Polym. Sci.*, **59**, 10 (2021); https://doi.org/10.1002/pol.20200721
3. D.A. Tomalia, H. Baker, J. Dewald, M. Hall, G. Kallos, S. Martin, J. Roeck, J. Ryder and P. Smith, *Polym. J.*, **17**, 117 (1985); https://doi.org/10.1295/polymj.17.117
4. S.M. Fatemi, S.J. Fatemi and Z. Abbasi, *Polym. Bull.*, **77**, 6671 (2020); https://doi.org/10.1007/s00289-019-03076-4
5. A. Janaszewska, J. Lazniewska, P. Trzepiński, M. Marcinkowska and B. Klajnert-Maculewicz, *Biomolecules*, **9**, 330 (2019); https://doi.org/10.3390/biom9080330
6. N. Shahini, F. Badalkhani-Khamseh and N.L. Hadipour, *J. Mol. Liq.*, **399**, 124396 (2024); https://doi.org/10.1016/j.molliq.2024.124396
7. P.K. Tripathi and S. Tripathi, in eds.: A. Chauhan and H. Kulhari, Dendrimers for Anticancer Drug Delivery, In: Pharmaceutical Applications of Dendrimers, Elsevier, Chap. 6, pp. pp. 131-150 (2020).
8. N.T. Pourianazar, P. Mutlu and U. Gunduz, *J. Nanopart. Res.*, **16**, 2342 (2014); https://doi.org/10.1007/s11051-014-2342-1
9. B.M. Johnston, A.J. Grodzinsky and P.T. Hammond, *Soft Matter*, **19**, 3033 (2023); https://doi.org/10.1039/D2SM01698B
10. K. Wu, B. Wang, B. Tang, L. Luan, W. Xu, B. Zhang and Y. Niu, *Chin. Chem. Lett.*, **33**, 2721 (2022); https://doi.org/10.1016/j.cclet.2021.08.126
11. X. Zhao, S.C.J. Loo, P.P.F. Lee, T.T.Y. Tan and C.K. Chu, *J. Inorg. Biochem.*, **104**, 105 (2010); https://doi.org/10.1016/j.jinorgbio.2009.10.001
12. L. Luan, B. Tang, S. Ma, L. Sun, W. Xu, A. Wang and Y. Niu, *J. Mol. Liq.*, **330**, 115634 (2021); https://doi.org/10.1016/j.molliq.2021.115634
13. Y. Zhou, L. Luan, B. Tang, Y. Niu, R. Qu, Y. Liu and W. Xu, *Chem. Eng. J.*, **398**, 125651 (2020); https://doi.org/10.1016/j.cej.2020.125651
14. S. Jain, M. Rana, R. Sultana, R. Mehandi and Rahisuddin, *Polycycl. Aromat. Compd.*, **43**, 6351 (2023); https://doi.org/10.1080/10406638.2022.2117210
15. E. Pahontu, M. Proks, S. Shova, G. Lupascu, S.-F. Barbuceanu, L.-I. Socea, D.-C. Ilies, M. Badea, V. Paunescu, D. Istrati, D. Draganescu, A. Gulea, and C.E.D. Pîrvu, *Appl. Organomet. Chem.*, **33**, e5185 (2019); https://doi.org/10.1002/aoc.5185
16. S.S. Shah, D. Shah, I. Khan, S. Ahmad, U. Ali and A.U. Rahman, *Biointerface Res. Appl. Chem.*, **10**, 6936 (2020); https://doi.org/10.33263/BRIAC106.69366963
17. Q.-U.-A. Sandhu, M. Pervaiz, A. Majid, U. Younas, Z. Saeed, A. Ashraf, R.R.M. Khan, S. Ullah, F. Ali and S. Jelani, *J. Coord. Chem.*, **76**, 1094 (2023); https://doi.org/10.1080/00958972.2023.2226794
18. A. Catalano, M.S. Sinicropi, D. Iacopetta, J. Ceramella, A. Mariconda, C. Rosano, E. Scali, C. Saturnino and P. Longo, *Appl. Sci.*, **11**, 6027 (2021); https://doi.org/10.3390/app11136027
19. S. Kaushik, S.K. Paliwal, M.R. Iyer and V.M. Patil, *Med. Chem. Res.*, **32**, 1063 (2023); https://doi.org/10.1007/s00044-023-03068-0
20. L. Lv, T. Zheng, L. Tang, Z. Wang and W. Liu, *Coord. Chem. Rev.*, **525**, 216327 (2025); https://doi.org/10.1016/j.ccr.2024.216327
21. G.G. Mohamed, M.M. Omar and A.M.M. Hindy, *Spectrochim. Acta A Mol. Biomol. Spectrosc.*, **62**, 1140 (2005); https://doi.org/10.1016/j.saa.2005.03.031
22. S.A. Shaikh, S.S. Bhat, V.K. Revankar, N. S, Mahesha, N.K. Loknath and V. Kumbar, *J. Coord. Chem.*, **76**, 1586 (2023); https://doi.org/10.1080/00958972.2023.2265037
23. S. Yavuz, D.A. Köse, S. Özkinali, D. Tatar and A. Veyisoglu, *J. Mol. Struct.*, **1322**, 140364 (2025); https://doi.org/10.1016/j.molstruc.2024.140364
24. M. Cangiotti, D. Staneva, M.F. Ottaviani, E. Vasileva-tonkova and I. Grabchev, *J. Photochem. Photobiol. Chem.*, **415**, 113312 (2021); https://doi.org/10.1016/j.jphotochem.2021.113312
25. R. Esfand and D.A. Tomalia, in eds. J.M.J. Fréchet and D.A. Tomalia, Laboratory Synthesis of Poly(amidoamine) (PAMAM) Dendrimers, Dendrimers and Other Dendritic Polymers, John Wiley & Sons, Ltd., Chap. 25, pp. 587-604 (2001).
26. C.B. Roy and J.S. Meshram, *J. Lumin.*, **171**, 208 (2016); https://doi.org/10.1016/j.jlumin.2015.10.059
27. J. Wang, H. Li, L. Song, W. Shi, N. Zhang and C. Li, *J. Macromol. Sci. A Pure Appl. Chem.*, **53**, 709 (2016); https://doi.org/10.1080/10601325.2016.1224629